Taylor & Francis
Taylor & Francis Group

Canadian Journal of Remote Sensing
Journal canadien de télédétection

ISSN: (Print) (Online) Journal homepage: https://www.tandfonline.com/loi/ujrs20

Deep Learning Approaches to Spatial Downscaling of GRACE Terrestrial Water Storage Products Using EALCO Model Over Canada

Hongjie He, Ke Yang, Shusen Wang, Hasti Andon Petrosians, Ming Liu, Junhua Li, José Marcato Junior, Wesley Nunes Gonçalves, Lanying Wang & Jonathan Li

To cite this article: Hongjie He, Ke Yang, Shusen Wang, Hasti Andon Petrosians, Ming Liu, Junhua Li, José Marcato Junior, Wesley Nunes Gonçalves, Lanying Wang & Jonathan Li (2021): Deep Learning Approaches to Spatial Downscaling of GRACE Terrestrial Water Storage Products Using EALCO Model Over Canada, Canadian Journal of Remote Sensing, DOI: 10.1080/07038992.2021.1954498

To link to this article: https://doi.org/10.1080/07038992.2021.1954498

Published online: 26 Jul 2021.

CANADIAN JOURNAL OF REMOTE SENSING
https://doi.org/10.1080/07038992.2021.1954498

Deep Learning Approaches to Spatial Downscaling of GRACE Terrestrial Water Storage Products Using EALCO Model Over Canada

Approches d'apprentissage en profondeur pour l'amélioration de la résolution spatiale des données du stockage d'eau terrestre GRACE à l'aide du modèle EALCO au Canada

Hongjie He[a], Ke Yang[b], Shusen Wang[c], Hasti Andon Petrosians[a], Ming Liu[a], Junhua Li[c], José Marcato Junior[d], Wesley Nunes Gonçalves[d,e], Lanying Wang[a], and Jonathan Li[a,b]

[a]Department of Geography and Environmental Management, University of Waterloo, Waterloo, ON, Canada; [b]Department of Systems Design Engineering, University of Waterloo, Waterloo, ON, Canada; [c]Canada Centre for Remote Sensing, Natural Resources Canada, Ottawa, ON, Canada; [d]Faculty of Engineering, Architecture and Urbanism and Geography, Federal University of Mato Grosso do Sul, Campo Grande, Mato Grosso do Sul, Brazil; [e]Faculty of Computer Science, Federal University of Mato Grosso do Sul, Campo Grande, Mato Grosso do Sul, Brazil

ABSTRACT

Estimating terrestrial water storage (TWS) with high spatial resolution is crucial for hydrological and water resource management. Comparing to traditional in-situ data measurement, observation from space borne sensor such as Gravity Recovery and Climate Experiment (GRACE) satellites is quite effective to obtain a large-scale TWS data. However, the coarse resolution of the GRACE data restricts its application at a local scale. This paper presents three novel convolutional neural network (CNN) based approaches including the Super-Resolution CNN (SRCNN), the Very Deep Super-Resolution (VDSR), and the Residual Channel Attention Networks (RCAN) to spatial downscaling of the monthly GRACE TWS products using the outputs of the Ecological Assimilation of Land and Climate Observations (EALCO) model over Canada. We also compare the performance of CNN-based methods with the empirical linear regression-based downscaling method. All comparison results were evaluated by root mean square error (RMSE) between the reconstructed GRACE TWS and the original one. RMSEs over the matched pixels are 22.3, 14.4, 18.4 and 71.6 mm of SRCNN, VDSR, RCAN and linear regression-based method respectively. Obviously, VDSR shows the best accuracy among all methods. The result shows all CNN-based super resolution methods preform much better than traditional method in spatial downscaling.

RÉSUMÉ

L'estimation du stockage d'eau terrestre (TWS) avec une haute résolution spatiale est cruciale pour la gestion des ressources hydrologiques et en eau. Par rapport aux mesures in situ traditionnelles, l'observation à partir de capteurs spatiaux tels que les satellites *Gravity Recovery and Climate Experiment* (GRACE) est assez efficace pour obtenir des données TWS à grande échelle. Cependant, la résolution grossière des données GRACE limite son application à une échelle locale. Cet article présente trois nouvelles approches basées sur les réseaux de neurones convolutifs (CNN), dont le *Super-Resolution* CNN (SRCNN), le *Very Deep Super-Resolution* (VDSR) et les *Residual Channel Attention Networks* (RCAN) pour l'amélioration de la résolution spatiale des GRACE TWS mensuels, produits utilisant les résultats du modèle d'assimilation écologique des observations terrestres et climatiques (EALCO) au Canada. Nous comparons également les performances des méthodes basées sur CNN avec la méthode empirique basée sur la régression linéaire. Tous les résultats de comparaison ont été évalués par l'erreur quadratique moyenne (RMSE) entre le GRACE TWS reconstruit et l'original. Les RMSE sur les pixels appariés sont respectivement de 22,3 mm, 14,4 mm, 18,4 mm et 71,6 mm pour SRCNN, VDSR, RCAN et la méthode basée sur la régression linéaire. De toute évidence, VDSR montre la meilleure précision parmi toutes les méthodes. De plus, toutes les méthodes de super résolution basées sur CNN se comportent bien mieux que la méthode traditionnelle de réduction d'échelle spatiale.

ARTICLE HISTORY
Received 28 June 2020
Accepted 30 June 2021

CONTACT Ke Yang ke.yang@uwaterloo.ca; Jonathan Li junli@uwaterloo.ca

Introduction

Terrestrial water storage (TWS) quantification and dynamic changes monitoring are crucial to comprehend the global and the local water cycle. TWS integrates various water components present in a terrestrial ecosystem, which include surface water (e.g. lakes, rivers, and snow), soil water, groundwater, and water contained in plants and organisms. The changes in each of these components can lead to TWS variations. TWS provides insights for sustainable water resources management, ecosystem productivity, and climate change.

There exists a wide range of methods and techniques for measuring the various components of TWS in terrestrial ecosystems, such as the radioactive technique (e.g. neutron probe) and capacitive technique (e.g. time-domain reflectometry TDR) for measuring soil water, and well monitoring using piezometers for measuring water-levels of groundwater. However, estimating TWS for a region is extremely difficult due to limitations in the quantity and quality of these observations and the heterogeneities and complexities of the soils and aquifers, which often constrain regional upscaling from the site measurements. To overcome this, NASA (National Aeronautics and Space Administration) and DLR (German Aerospace Center) launched the Gravity Recovery and Climate Experiment (GRACE) mission in 2002, providing monthly TWS variation information over a long period at a global scale. GRACE observations have been widely adopted to understand the temporal trends in TWS at regional and global scales (Fok and He 2018; Frappart et al. 2013; Kordpour et al. 2019; Lezzaik and Milewski 2018; Li et al. 2016; Shamsudduha et al. 2017; Voss et al. 2013; Wang and Li 2016), characterize river flows (Riegger and Tourian 2014; Sproles et al. 2015; Macedo et al. 2019; Wang 2019) and hydrologic extremes such as drought (Leblanc et al. 2009; Ma et al. 2017; Thomas et al. 2014) and flood (Reager and Famiglietti 2009; Reager et al. 2014; Wang and Russell 2016; Wang et al. 2017), and quantify evapotranspiration changes (Long et al. 2014; Muskett and Romanovsky 2009).

The significant limitations of GRACE-based TWS data include their coarse spatiotemporal resolutions (monthly and over 330 km) and the vertical integration of the water storage components. Improving the resolution of GRACE data would significantly enhance information availability, especially for local-scale studies, which could also provide data support for regions with few in-situ monitoring facilities. Downscaling methods to convert the large-scale low-resolution (including both spatial and temporal scales) data into the small-scale and high-resolution products have drawn the attention of researchers (Chen et al. 2019). The term downscaling used in this paper refers to an increase in spatial resolution, while upscaling refers to a decrease in spatial resolution. Previous studies have shown the capability of high-resolution physical models for downscaling (Eicker et al. 2014; Gustafsson et al. 2018; Lee et al. 2017). These models are resource-intensive in terms of computational resources and expertise. Statistical downscaling based on historical observations to establish the relationships between coarse and fine resolution observations, in contrast, requires few auxiliary data and less computation time (Jing et al. 2016; Yin et al. 2018). Therefore, statistical methods have been preferred to improve the spatial resolution of GRACE TWS data.

Given the optimal performance of machine learning-based methods in computer science, there is an increasing number of studies adopting these advanced statistical methods to establish the relationship between low-resolution and high-resolution images in geoscience and climate science (Rahaman et al. 2019). Machine learning algorithms, such as boosted regression tree (Milewski et al. 2019), random forests (Chen et al. 2019), and time-lagged feed-forward neural network (TLFN) (Coulibaly et al. 2005), were widely used in spatial or temporal downscaling and showed satisfactory performance. However, features are essential for model training and must be manually selected with specific prior knowledge.

Many papers have proved that CNN-based deep learning methods performed better than traditional machine learning methods in downscaling image resolution (Schoof and Pryor 2001; Tomassetti et al. 2009; Sun 2013; Schmidhuber 2015; Alexakis and Tsanis 2016; Miro and Famiglietti 2018; Salimi et al. 2019), such as ANN-based methods (Shi et al. 2016; Rocha Rodrigues et al. 2018; Baño-Medina et al. 2020). Deep learning algorithms seek to automatically explore the input-output relationship from data, where the whole learning process can be considered as an entirety (Song and Lee 2013). Thus, the SRCNN (Dong et al. 2016) has been broadly applied in geoscience data downscaling. For example, Ducournau and Fablet (2016) applied SRCNN to downscale satellite-based sea surface temperature (SST) data. They verified that SRCNN outperformed the bicubic interpolation and other traditional approaches such as linear Empirical Orthogonal Function (EOF) Linear-EOF and SVR-EOF methods for geophysical data downscaling. Vandal et al. (2017) developed a generalized stacked

SRCNN framework with auxiliary data, which named Deep Statistical Downscaling (DeepSD). DeepSD can statistical downscale the daily precipitation data over the Continental United States from 100 to 12.5 km with accepted accuracy. They also reported that heterogeneous spatial areas can be downscaled by a single trained model, and the deep learning method performed better than traditional methods.

Apart from commonly used SRCNN as mentioned above, there are many other CNN-based methods developed for image resolution enhancement. Those methods are defined as single image super resolution (SISR) methods. Following SRCNN, the first CNN-based image super resolution method (Dong et al. 2016), many other deep learning-based images super resolution methods were proposed. Fast super-resolution CNN (FSRCNN) was proposed to improve the efficiency of SRCNN, with the help of deconvolution layer (Dong et al. 2016). Shi et al. (2016) proposed an efficient Sub-Pixel Convolutional Neural Network (ESPCN) with sub-pixel convolutional layer to construct a better super resolution method. Some researchers proposed other methods to improve deep learning, such as Very Deep Super-Resolution (VDSR) (Kim et al. 2016a), Deeply Recursive Convolutional Network (DRCN) (Kim et al. 2016b), Residual Encoder-Decoder Networks (RED-Net) (Mao et al. 2016). Inspired by VDSR and DRCN, Deep Recursive Residual Network (DRRN) was proposed, which combined global residual learning from VDSR, local residual learning from ResNet (Residual Network) (He et al. 2016) and recursive learning from DRCN (Tai et al. 2017). With transposed convolutional layers and a robust loss function, Laplacian Pyramid Super-Resolution Network (LapSRN) was proposed (Lai et al. 2017). Dense block and generative adversarial network were also introduced in SISR field soon, which led to the proposal of SRDenseNet (Tong et al. 2017) and super-resolution generative adversarial network (SRGAN) (Ledig et al. 2017). Enhanced deep super-resolution network (EDSR) and multi-scale deep super-resolution system (MDSR) were proposed by simplifying ResNet architecture in SRGAN, which outperform all previous methods (Lim et al. 2017). Attention mechanism distributes more processing resources to part of model input which include more useful information. Take channel-wise attention mechanism into SISR applications, researcher proposed very deep Residual Channel Attention Networks (RCAN) (Zhang et al. 2018). Further, Second-order Attention Network (SAN) with second-order channel attention (SOCA) mechanism was proposed to generate better results in image super resolution applications (Dai et al. 2019). In recent literatures, Residual Feature Aggregation Network (RFANet), which was proposed with a general residual feature aggregation (RFA) framework, outperform all exist CNN based image super resolution methods (Liu et al. 2020). Consequently, advanced image super resolution methods were developed in recent years. However, the applications of these methods are under explored in geoscience.

Besides, according to most references, all CNN based methods were used to downscale general images with the up-sampling factor of 2, 3, 4 and, sometimes, 8. All methods can be used in geoscience successfully with adaption operations. However, in geoscience, the scale factors may be different. In this study, we targeted on the first and easiest CNN-based super resolution method SRCNN, the first batch deeper network VDSR, and the first attention mechanism involved network RCAN to test the viability of CNN-based super resolution methods of downscaling geoscience data with a large-scale factor. SRCNN has shown higher performance than that of conventional methods (Dong et al. 2016; Ducournau and Fablet 2016). Meanwhile VDSR and RCAN also showed good performance in resolution enhancement of remote sensing images (Shermeyer and Van Etten 2019; Chen et al. 2020). But in this work, we focus on evaluating the performance of CNN-based methods to larger scale factor in the TWS data downscaling. Due to the availability of the auxiliary data, the linear regression method and bicubic interpolation were selected and implemented as conventional methods in the comparative study.

Moreover, higher resolution ground truth data is an essential element to train the CNN-based models in downscaling applications. In this study, the ground truth is set as the water storage outputs of the Ecological Assimilation of Land and Climate Observations (EALCO) model which developed by Natural Resources Canada (NRCan). The rest of the paper is structured as follows: Section "Data and Data Processing" describes the data and data preprocessing applied in our research. Section "Method" describes our method. Section "Results" presents the results. Section "Discussion" discusses the results obtained. Section "Conclusion" concludes the paper.

Data and data processing

EALCO model

The EALCO model is a land surface model developed for simulating terrestrial ecosystem physical, physiological and biogeochemical processes using in situ and

remote sensing observations. The model includes five major modules for simulating land surface radiation transfer, energy balance, water dynamics, and carbon and nitrogen biogeochemical cycles (Wang et al. 2007; Wang 2008; Wang et al. 2013). The water storage changes in EALCO is obtained by simulating the terrestrial water cycle processes which include (1) canopy evapotranspiration which includes leaf transpiration and canopy evaporation or sublimation from intercepted rain, snow, dew, or frost; (2) soil evaporation and snow sublimation at the ground surface; (3) open water surface evaporation from lakes and rivers; (4) plant root water uptake and plant water storage; (5) soil water transfers and soil water-groundwater interactions; (6) snow processes which use dynamic snow layering schemes for snow freeze and thaw simulations (Zhang et al. 2008). The water module is dynamically coupled with the other four modules in EALCO to integrate the dynamic controls of atmosphere, and plant and soil conditions in the ecosystem water cycle.

The EALCO model performance has been tested over a wide range of ecosystems in several modeling studies, including the Boreal Ecosystem-Atmosphere Study (BOREAS) (Amthor et al. 2001; Potter et al. 2001), the AmeriFlux Network (Hanson et al. 2004), the Fluxnet-Canada Research Network (FCRN) (Grant et al. 2005, 2009, 2006), and the free-air CO_2 enrichment (FACE) model-data synthesis study (De Kauwe et al. 2014; Zaehle et al. 2014; Walker et al. 2014; Medlyn et al. 2015). Recent assessments of EALCO water results were conducted by examining water budget closures for all gauged watersheds in Canada (Wang, McKenney, et al. 2014; Wang, Huang, et al. 2014; Wang, Huang, et al. 2015), and by comparing it with results from other land surface models including the common land model (CLM) and variables infiltration capacity (VIC), in situ observations, and remote sensing products for the entire landmass of Canada (Wang, Pan, et al. 2015). Developed in Canada, the EALCO model includes comprehensive algorithms, particularly for simulating cold region water and energy transfer processes. The EALCO has demonstrated its robustness in the tests mentioned previously, and it provides confidence for its effective application in this study.

EALCO is driven by meteorological variables of shortwave and longwave radiation, air temperature and humidity, precipitation, wind speed, and atmospheric pressure. It runs at a half-hourly time step, and the spatial resolution is determined from the remote sensing data inputs (Toth and Jóźków 2016). In this study, the EALCO (V4.2) water content, which includes soil water, snow water equivalent, and plant water, is used. These data products are at 5 km spatial resolution under Canada Lambert Conformal Conic (CanLCC) projection, covering the entire landmass of Canada. The EALCO monthly water content is calculated from the 30-minute water content based on the actual days used for each GRACE monthly solution. Since the GRACE TWS data are anomalies relative to the baseline average over a specific time period, we calculated the EALCO water content anomalies by subtracting the time-mean baseline over the period of April 2002 to December 2016 to make EALCO and GRACE data comparable. The EALCO monthly water content anomalies dataset is referred to as the EALCO TWS for the rest of the paper. Figure 1a and 1b show

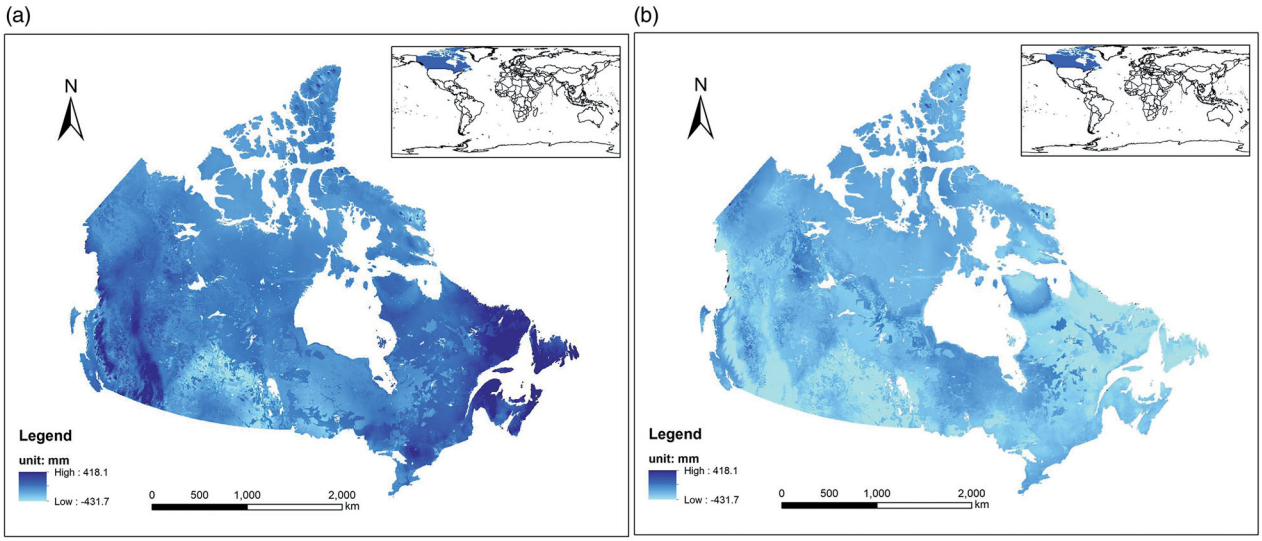

Figure 1. Spatial distribution of EALCO TWS data in (a) April 2003 and (b) October 2003 with a spatial resolution of 5 km.

examples of the EALCO TWS in April and October of 2003, respectively, which were the time with maximum and minimum TWS values in most regions of Canada (Wang and Li 2016).

GRACE

In this study, the GRACE Level-3 monthly TWS global product, processed by the Jet Propulsion Laboratory (JPL), was downloaded from the JPL website (https://podaac.jpl.nasa.gov). The dataset was processed from the release RL06 spherical harmonics and provided at a $1^\circ \times 1^\circ$ global grids (Cooley and Landerer 2019). The monthly TWS data are anomalies to the baseline average over January 2004 to December 2009. Within the dataset's timespan of April 2002 to June 2017, there were 16 months without data which include June, July 2002, June 2003, January, June 2001, May 2012, March, September 2013, February 2014, May, October, November 2015, April, September, October 2016 and February 2017. In this study, we adjusted the GRACE TWS data baseline to the average of April 2002 to December 2016 to make it be comparable to the EALCO TWS. The data was then subset to cover the landmass of Canada by using a shapefile of Canada national boundary in the "Regionmask" module (https://anaconda.org/conda-forge/regionmask) in Python. The subset data was reprojected to the CanLCC projection at 110 km spatial resolution by using ArcGIS (V10.6) program, in which the nearest neighbor resampling was used to match the projection of the EALCO TWS data. Figure 2 shows two sample images of the GRACE TWS in April and October of 2003 at 110 km resolution under the CanLCC projection. Figures 1 and 2 show similar spatial-temporal distributions of TWS in Canada. Indeed, the GRACE TWS data has been proven to be in good agreement of spatial and temporal variations with TWS derived from land surface models (Long et al. 2015; Ning et al. 2014; Seyoum and Milewski 2016).

Method

Conventional downscaling methods

As aforementioned, the EALCO output corresponds to GRACE TWS with different spatial and temporal resolutions. In this study, we first implement the pixel-wised and linear regression-based method as the baseline to downscale GRACE TWS. This method was used by Alexakis and Tsanis (2016) in their research. Since CNN-based downscaling methods cannot downscale more than 12 times (Vandal et al. 2017). To generate highest spatial resolution data, in our work, we selected 11 as the downscaling ratio in our work. Figure 3 shows the procedure for the linear regression-based downscaling. The detailed steps of EALCO-based GRACE TWS downscaling are given as follows:

- Upscaling the EALCO TWS data from 5 to 110 km using the arithmetic mean to match the spatial resolution of GRACE TWS data product;
- Establishing the relationship between EALCO 110 km TWS and GRACE 110 km TWS for each pixel. There are 784 pixel-based linear regressions in total over the study area after upscaling. The determination coefficient (R^2) and p-value for F and Student's t test were recorded;

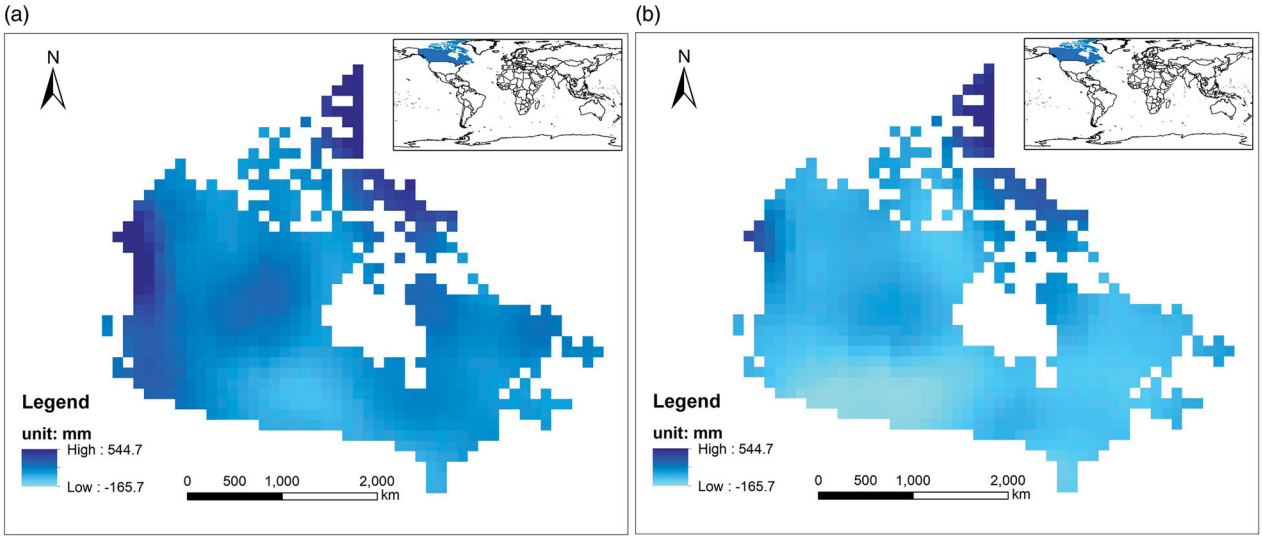

Figure 2. Sample of grided GRACE TWS images in (a) April 2003 and (b) October 2003 with 110 km spatial resolution used in this work.

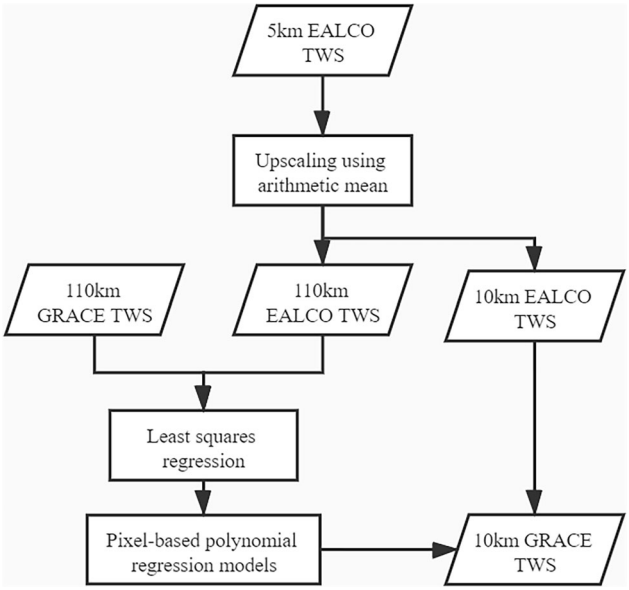

Figure 3. Flowchart of linear regression-based spatial downscaling model.

- Calculating final monthly 10 km TWS by applying the GRACE-EALCO TWS regressions to the 10 km EALCO TWS, upscaled from the 5 km EALCO TWS. For pixels in the boundary area with no corresponding GRACE pixel and regression equations, the average coefficient of 784 valid regressions was applied to those boundary pixels;
- Upscaling the downscaled GRACE TWS products to determine the uncertainty of the method. Here, averaging neighborhood pixels were used to upscale or reconstruct GRACE TWS at 110 km resolution. The root mean squared error (RMSE) was adopted to quantify the uncertainty:

$$\mathrm{RMSE} = \sqrt{\frac{1}{N}\sum_{i=1}^{N}(observed_i - predicted_i)^2} \quad (1)$$

where $observed_i$ and $predicted_i$ are original 110 km resolution GRACE TWS, and downscaled and then reconstructed GRACE TWS, respectively. N here is the number of pixels used for calculating RMSE in 158 months.

In super-resolution field, Peak Signal-to-Noise Ratio (PSNR) and Structural Similarity Index Measure (SSIM) (Shermeyer and Van Etten 2019) are mostly employed as metrics to evaluate and compare different methods. In remote sensing, Cumulative Probability of Blur Detection (CPBD) (Keshk et al. 2014) and Feature Similarity Index Measure (FSIM) (Chen et al. 2020) were also applied along with PSNR and SSIM. However, the missing of high spatial resolution GRACE TWS, as well as other types of ground truth data, makes it impossible to use these metrics here. In an alternative way, we used RMSE in this study to evaluate and compare different downscaling methods by considering the information loss in downscaling. Since bicubic interpolation is widely used in super-resolution for pre-processing and baseline. Thus, apart from linear regression, we also used bicubic interpolation method to downscale GRACE TWS.

CNNs-based downscaling

Super-resolution CNNs

The SRCNN architecture was considered as the benchmark of deep architecture for single image super-resolution (Yang et al. 2019). Figure 4 shows the overall architecture of SRCNN. SRCNN model includes patch extraction and representation (Equation (2)), non-linear mapping (Equation (3)), and reconstruction (Equation (4)) steps by different convolutional layer. Thus, the formulation of the SRCNN can be envisaged as an ordinary CNN that approximates the low-resolution images and high-resolution images (LR-HR) mapping in an end-to-end manner.

Before inputting LR images into the SRCNN network, the LR input needs to be resampled to the desired size using the bicubic interpolation (Dong et al. 2016). The patch extraction part is expressed as the following convolutional layer that receives an image Y as input:

$$\mathrm{F_1(Y)} = \max(0, \mathrm{W_1} * \mathrm{Y} + \mathrm{B_1}) \quad (2)$$

where $\mathrm{W_1}$ and $\mathrm{B_1}$ are the filters and biases, and $*$ denotes the convolution operation. In this work, $\mathrm{W_1}$ is composed of 64 filters of size $1 * 9 * 9$. Here, 1 is the channel of the input image and 9*9 is the filter size. $\mathrm{W_2}$ and $\mathrm{W_3}$ below were also presented in the manner of c * f * f, where c stands for channels or the dimension of feature maps in last layer. f * f stands for the filter size. The output is a feature map composed of a 64-dimensional feature for each patch.

The second part applies a non-linear mapping of the features of each patch using:

$$\mathrm{F_2(Y)} = \max(0, \mathrm{W_2} * \mathrm{F_1(Y)} + \mathrm{B_2}) \quad (3)$$

where $\mathrm{W_2}$ and $\mathrm{B_2}$ represents 32 filters of size $64 \times 1 \times 1$ and biases, respectively.

Finally, the third part reconstructs the high-resolution image using a convolutional layer:

$$\mathrm{F(Y)} = \mathrm{W_3} * \mathrm{F_2(Y)} + \mathrm{B_3} \quad (4)$$

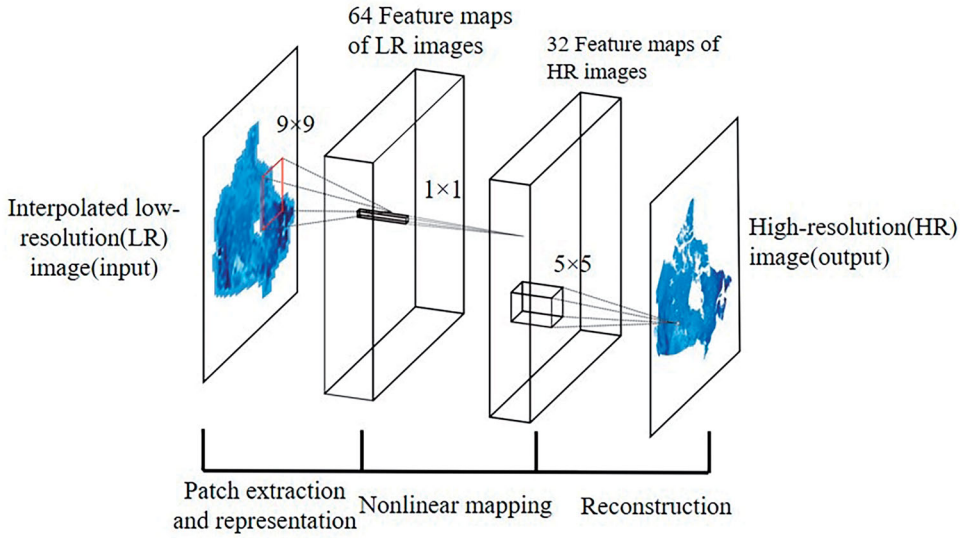

Figure 4. Architecture of the SRCNN network.

where W_3 and B_3 are the filters and biases, respectively. Here, we adopt only one filter of size $32 \times 5 \times 5$ to achieve the desired output image with one channel.

For training and optimizing the SRCNN, the mean square error (MSE) was used as the loss function. This loss function can be expressed as:

$$L(\Theta) = \frac{1}{n}\sum_{i=1}^{n} \|F(Y_i;\Theta) - X_i\|^2 \quad (5)$$

where X refers to the ground truth HR image, and Y refers to the bicubic upscaled version of LR image. Here, $\Theta = \{W_1, W_2, W_3, B_1, B_2, B_3\}$. F (*) refers to the mapping from LR to HR. Thus, $F(Y_i;\Theta)$ refers to the resulting HR image.

VDSR (Kim et al. 2016a) is developed based on SRCNN by making CNN deeper, which has a similar architecture to SRCNN. The difference between these two methods mainly lies into the number of hidden layers and the size of filters. In VDSR, 20 standard convolutional layers, each of them is composed of 64 3*3 kernels, are employed to translate images from LR to HR.

RCAN (Zhang et al. 2018) involved attention mechanism and residual learning into super-resolution. RCAN includes four parts: shallow feature extraction, deep feature extraction, downscaling module and reconstruction module, which correspond to patch extraction and representation, nonlinear mapping and reconstruction in SRCNN. Apart from the residual in residual (RIR) used in deep feature extraction and channel attention scheme, the most important part of RCAN is the upscale module differing from SRCNN and VDSR, which is developed based on ESPCN (Shi et al. 2016). With this module, the input of super-resolution model is smaller than which in SRCNN and VDSR. Consequently, CNN based super-resolution model can run more efficient without complex data preprocessing.

The detail of implementation

Figure 5 shows the flowchart of the SRCNN-based downscaling approach, which is as same as that of the VDSR-based downscaling approach. The RCAN-based approach has a similar one except the data pre-processing for input as circulated in red boxes (Figure 5)

Data processing. Firstly, the 10 km HR EALCO data simulated to a low spatial resolution (110 km) using the bicubic algorithm. The input training dataset of SRCNN and VDSR requires the same size of LR and HR pair. Because the original study of SRCNN and VDSR used bicubic to construct the same size of LR and HR pairs (Dong et al. 2016; Kim et al. 2016a). Then, the interpolated 110 km EALCO data then downscaled to 10 km by bicubic interpolation again to generate a LR input for SRCNN model training. Note that test dataset needs similar pre-processing in evaluation step.

The preprocessed EALCO data in all 158 months was tiled into 66*66 pixels with a stride of 28 pixels to accelerate the training process and increase the training data volume. As a result, we got 42,660 tiles with correspondent 10 km EALCO data as true value. After shuffling, those tiles were divided into training dataset (38,394 tiles) and validation dataset (4,266 tiles). To save all images without information loss, we saved all tiles into one h5 file. Therefore upon, the

training dataset and the validation dataset were prepared for training SRCNN and VDSR model.

Different from SRCNN and VDSR, in the RCAN training process, preparing training data is simpler. The input LR data are not required to resample to match the size of HR data pair. The original GRCAE TWS with the size of 44*52 can be directly used as input for downscaling. To match the number of samples for training each model, data augmentation, including width and height shifting, zooming, rotation, shearing, horizontal flipping is applied in training data preparation. After shuffling, the 640 tiles and 64 tiles prepared data is used for training and validation data in RCAN model.

Training process. For SRCNN and VDSR, 1e-5 and 128 were used as the learning rate and the batch size, respectively. For RCAN, we apply a learning rate of 1e-4 and batch size of 16 given the complex architecture and huge number of parameters. All models are reimplemented using TensorFlow and trained for 10,000 epochs. A single GPU of TITAN XP and CUDA 11.0 were used to support both model training and testing.

As we explained at the end of Section "Downscaling results using conventional methods", because we have no HR GRACE TWS, we adopt RMSEs to evaluate and compare different methods in this work. The spatial distribution of the deviation between reconstructed 110 km GRACE TWS and the original 110 km GRACE TWS was also calculated to show the uncertainty of different methods.

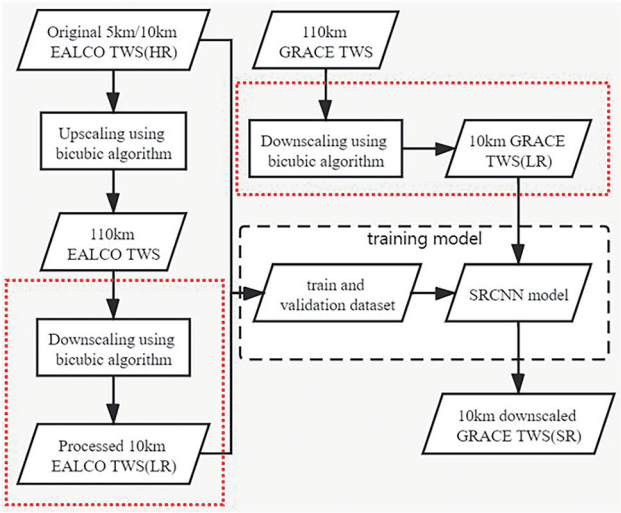

Figure 5. Flowchart of the SRCNN-based downscaling approach.

Results

In this section, we are going to present all the comparison and quantitative evaluation results of each method.

Downscaling results using conventional methods

Figures 6 and 7 show the upscaled ~110 km EALCO TWS maps and the downscaled 10 km GRACE TWS maps, respectively. As shown in Figure 7, the downscaled GRACE products presented more detailed information compared to the original GRACE data, the spatial pattern of which is generally consistent with that of EALCO TWS data (compared with Figure 3).

We adopted model-fitting R^2 to evaluate the performance of the EALCO-GRACE relationship for each pixel. Figure 8 shows the spatial pattern of R^2 over Canada. The regressions performed better in the west

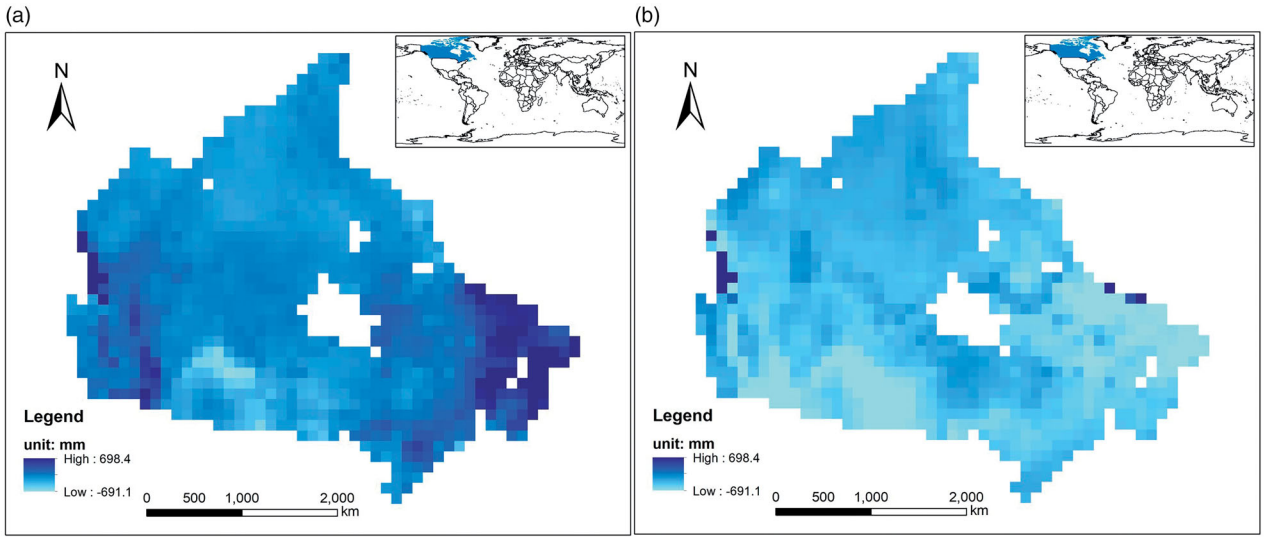

Figure 6. Spatial distribution of EALCO TWS data in (a) April 2003 and (b) October 2003 with a spatial resolution of 110 km.

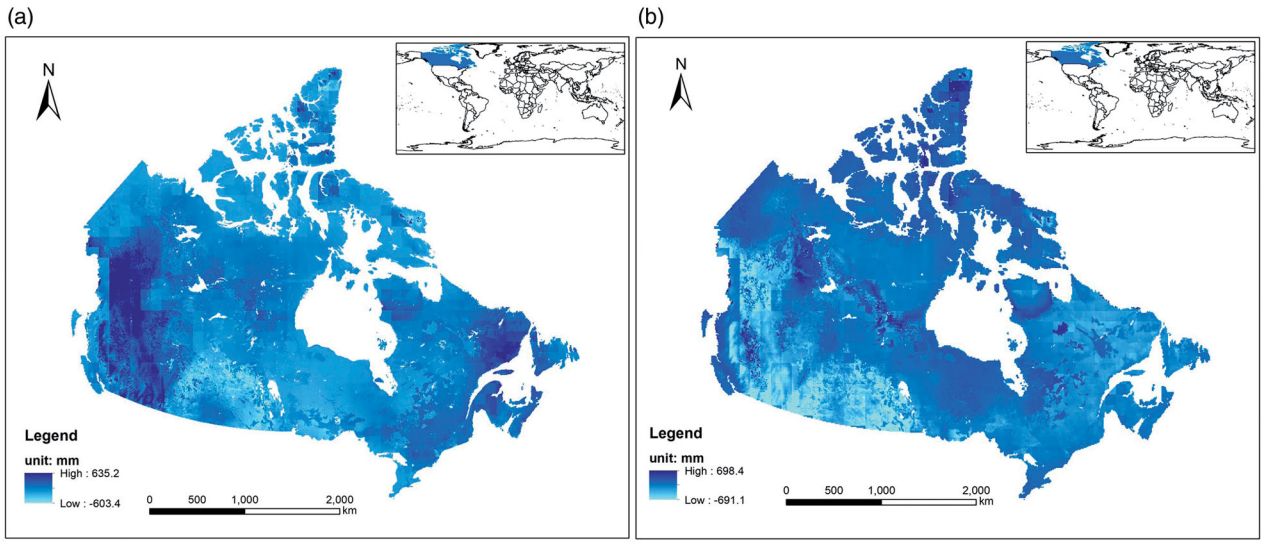

Figure 7. Spatial distribution of downscaled GRACE TWS data in (a) April 2003 and (b) October 2003 with a spatial resolution of 10 km.

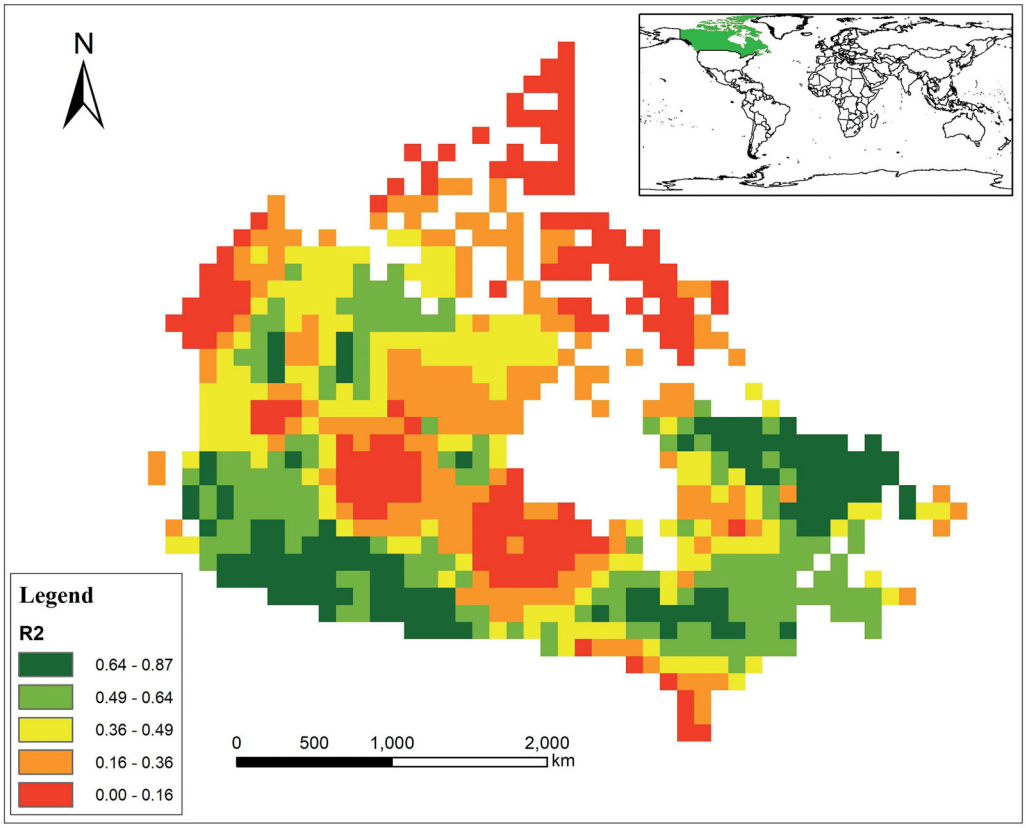

Fig. 8. Spatial distribution of R^2.

and east Canada than in other areas. Except for a few pixels in the north, most of the correlations are statistically significant through Student's *t*-test and *F*-test analysis, with both p-values less than 0.05 (Figure 9). As mentioned in Section "Results", we upscaled the result of downscaled 10 km GRACE TWS data back to 110 km spatial resolution for evaluating the uncertainty of our estimates (Figure 10). The RMSE between reconstructed 110 km GRACE TWS and original 110 km GARCE TWS for the linear regression-based downscaling method are 71.6 mm for valid pixels (N equals the number of matched pixels in each month, which is 158*784), indicating an acceptable performance of the downscaled method. Beside

we also plotted the spatial distribution of the deviation between the reconstructed GRACE TWS data and original GRACE TWS data (Figure 11). As shown in Figure 11, most deviation values lie in the range of $-100-10$ or $10-100$.

In addition, this study also implemented bicubic interpolation to downscale the GRACE TWS. The RMSE was 82.02 mm, which showed an inferior performance than linear regression.

CNN-based downscaling results

In this study, the CNN-based super-resolution methods were established for resolution enhancements of factors to 11, thereby generating a 10 km resolution TWS product. Figure 12 shows the training process. Blue lines and orange lines represent the learning curves of training and validation, respectively.

Figure 13 shows the downscaled GRACE TWS data output from SRCNN, VDSR and RCAN. The accuracy of the trained model was evaluated using the test dataset. For SRCNN, VDSR and RCAN, RMSEs between reconstructed 110 km GRACE TWS (Figure 14) and original 110 km GRACE TWS are 22.3, 14.4, and 18.4 mm for valid pixels (784*158), respectively. Here, arithmetic mean was used again to reconstruct 110 km GRACE TWS. Figure 15 shows the spatial distribution of the deviation of reconstructed and

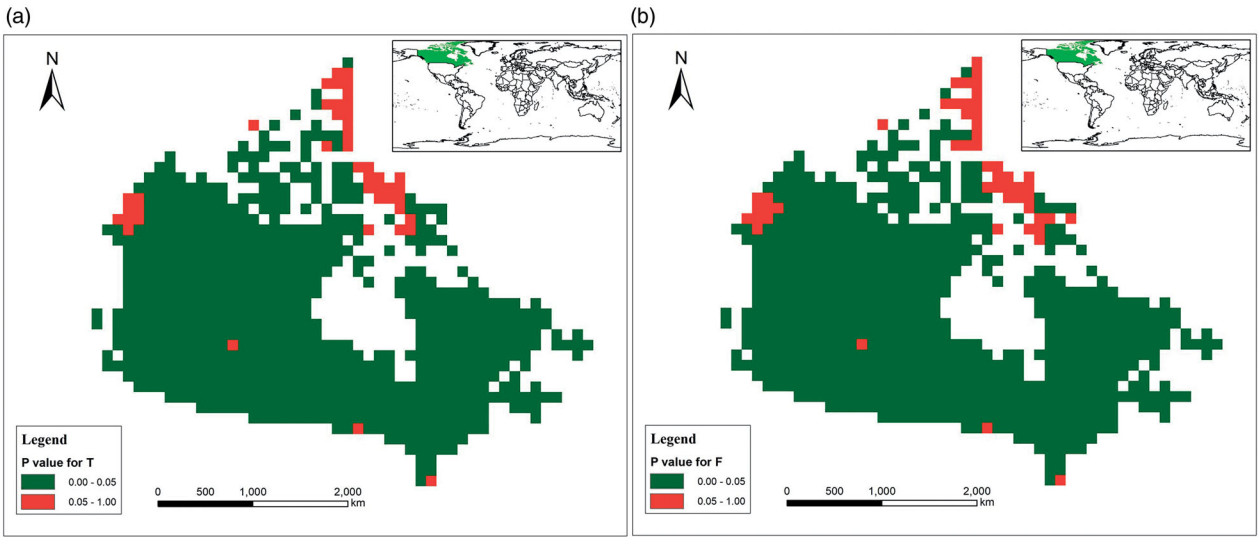

Figure 9. Spatial distribution of *p*-values for (a) Student's *t*-test and (b) *F*-test of all linear regression equations.

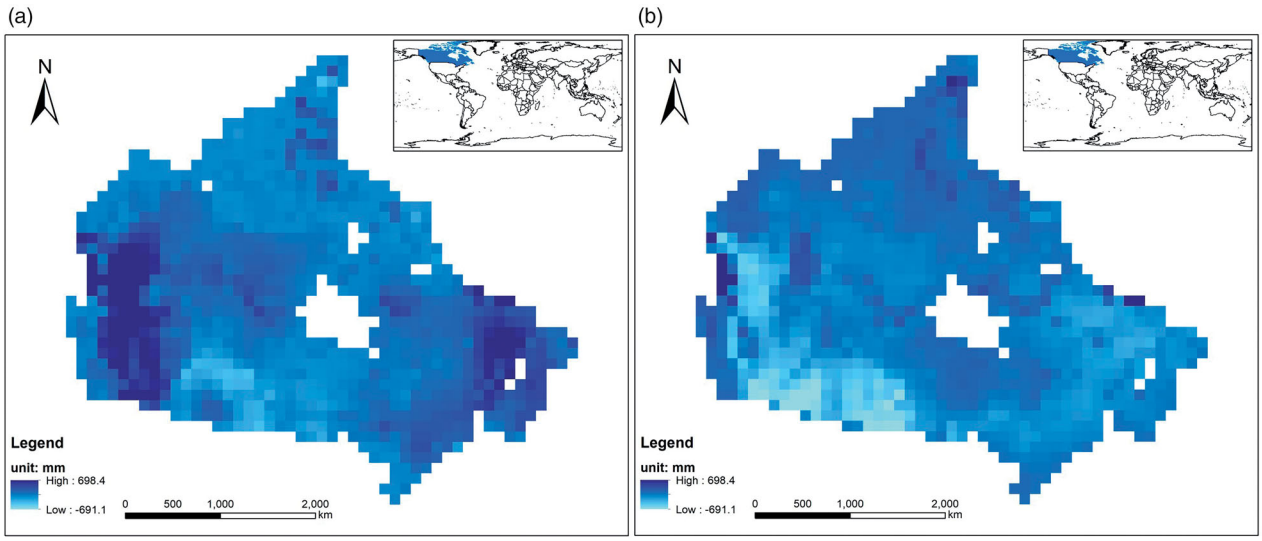

Figure 10. Spatial distribution of reconstructed GRACE TWS in (a) April 2003 and (b) October 2003 with a spatial resolution of 110 km.

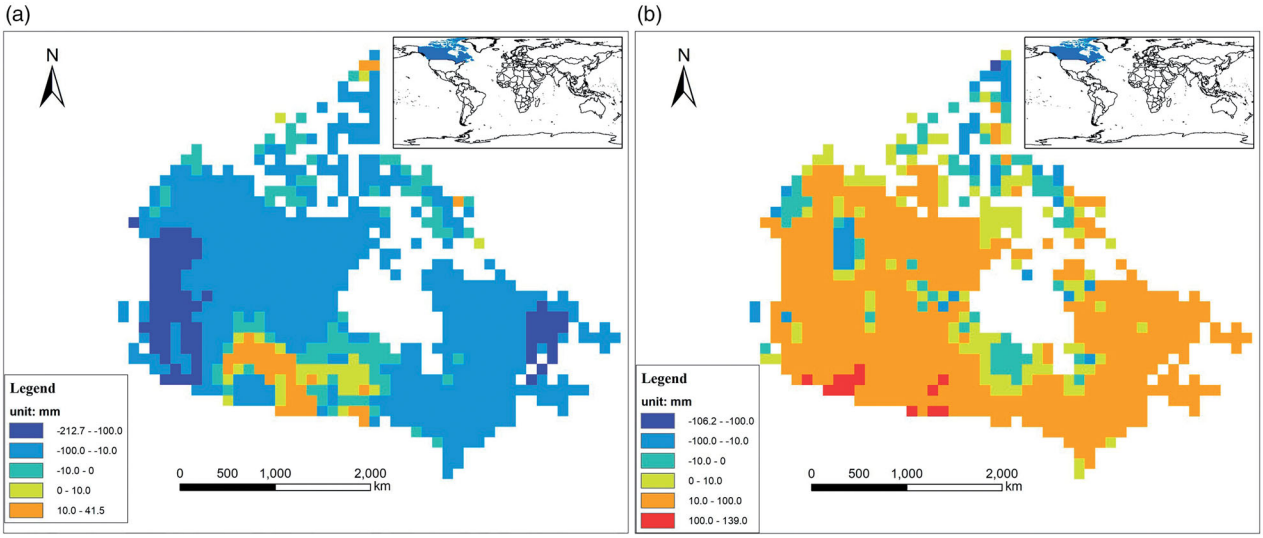

Figure 11. Spatial distribution of the deviation between reconstructed GRACE TWS data and original GRACE TWS data in (a) April 2003 and (b) October 2003(b) with a spatial resolution of 110 km.

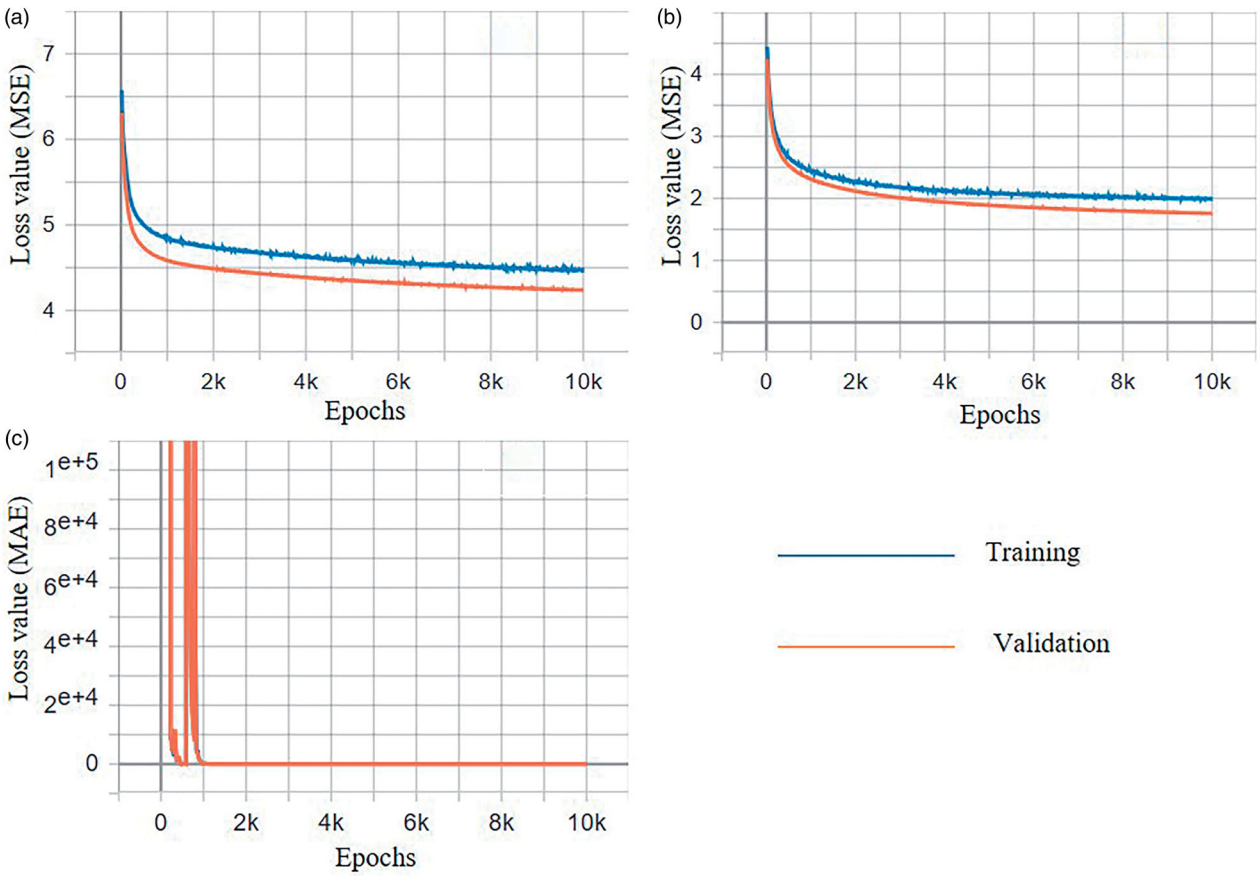

Figure 12. Training and validation learning curves: (a) SRCNN, (b) VDSR, (c) RCAN.

original GRACE TWS data. Most CNN-based results distributed in the range of $0 \sim 10$ and $-10 \sim 0$, which are significantly lower than the results linear regression.

Discussion

We adopted both a traditional statistical method and deep learning techniques to downscale the spatial resolution of GRACE TWS data. This study

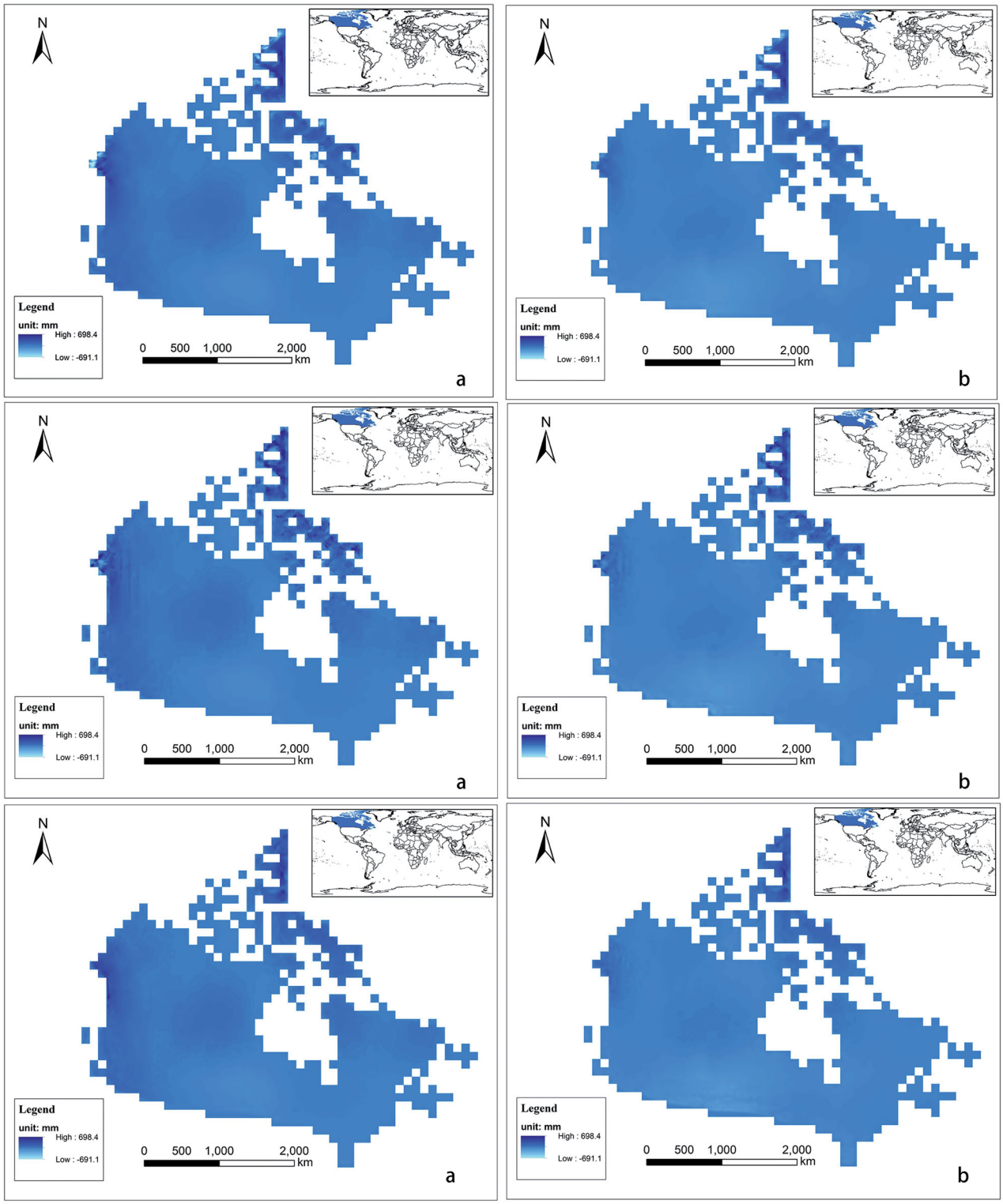

Figure 13. Spatial distribution of downscaled GRACE TWS data in (a) April 2003 and (b) October 2003 with a spatial resolution of 10 km, output from SRCNN (top), VDSR (middle) and RCAN (bottom).

demonstrated that CNN-based methods are more suitable for TWS downscaling process than conventional methods.

A linear regression-based spatial downscaling method was used to compare with deep learning approaches in this study. Considering the spatial heterogeneity of TWS, we established the EALCO-GRACE relationships for each pixel at 110 km resolution over Canada. The research was conducted based on the assumption that the relationships

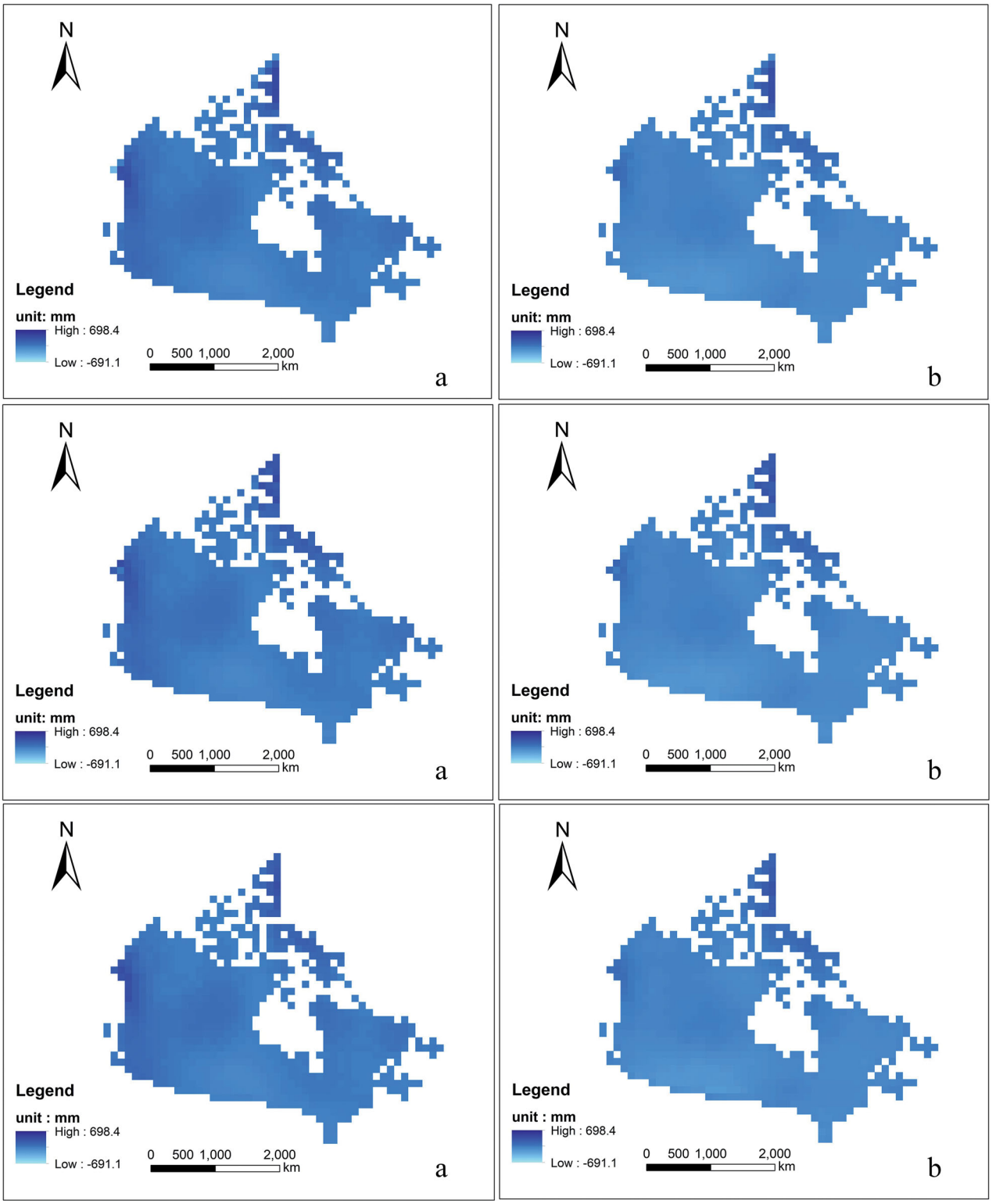

Figure 14. Spatial distribution of reconstructed GRACE TWS in (a) April 2003 and (b) October 2003 with a spatial resolution of 110 km, reconstructed using SRCNN (top), VDSR (middle), and RCAN (bottom).

between EALCO TWS and GRACE data remain stable over the period. The linear regression results for spatial downscaling in our research show an acceptable accuracy for most of Canada, with an overall average R^2 of 0.397 and relatively low RMSE. Both F test and Student's *t*-test also indicate the feasibility of the linear regression method. However, conspicuous Mach bands can be observed in the outputs. It may be caused by adopting the same regression formulas in 11×11 pixels in EALCO data to generate downscaled

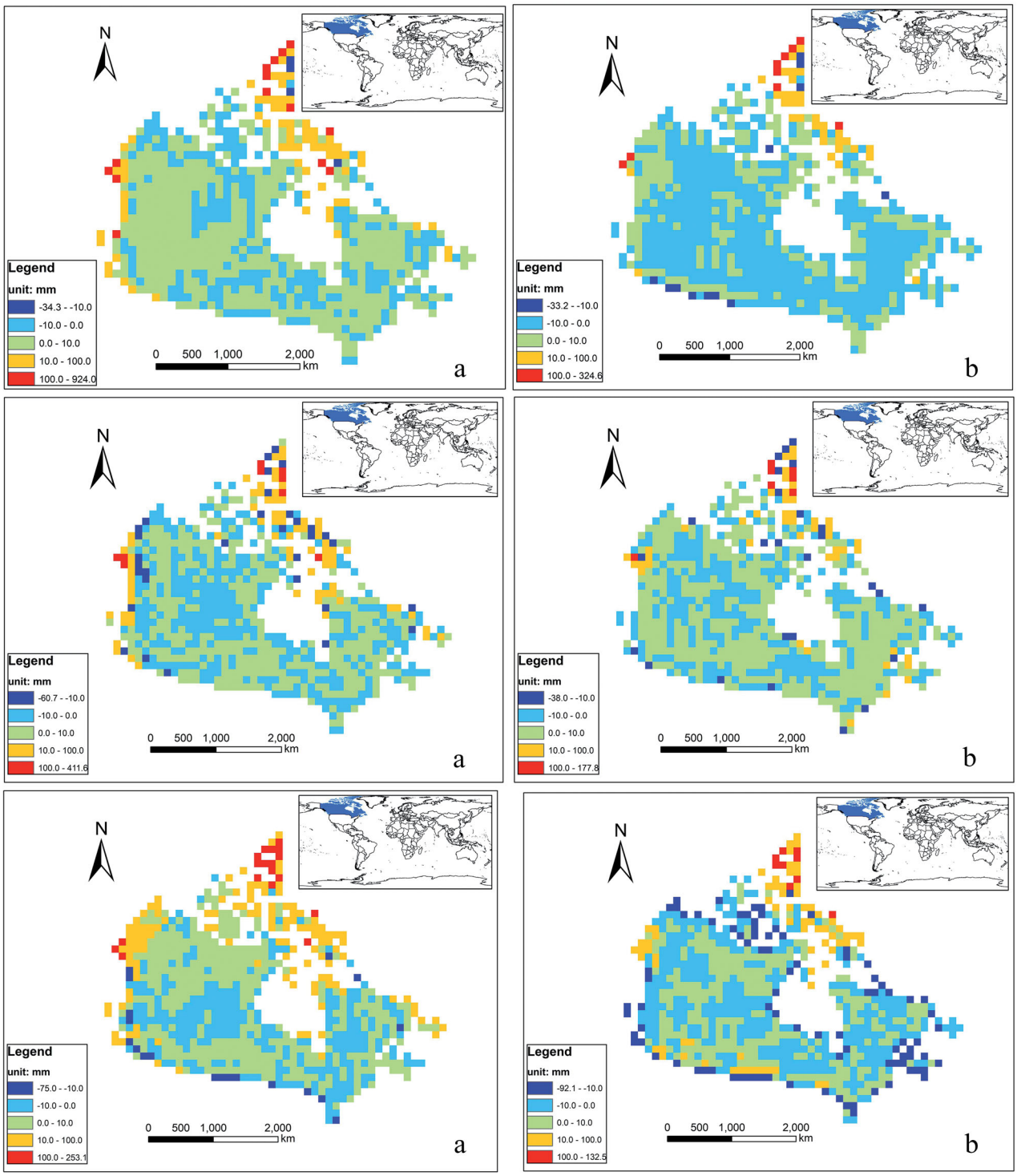

Figure 15. Spatial distribution of the deviation between reconstructed GRACE TWS data and original GRACE TWS data in (a) April 2003 and (b) October 2003 with a spatial resolution of 110 km, generated using SRCNN (top), VDSR (middle) and RCAN (bottom).

Table 1. Accuracy-efficiency analysis among CNN-based super-resolution methods.

Method	RMSE (mm)	Training time (hours)	Trainable parameters
SRCNN	22.3	28	8129
VDSR	14.4	280	665,921
RCAN	18.4	106	20,572,035

GRACE TWS data. In contrast, in some regions, the same formula may not be able to represent the relationship between EALCO TWS data and GRACE TWS data. As shown in Figure 13, some areas such as the westernmost region of Canada, and the Arctic Circle, exist some unexpected noisy pixels of the CNN-based results. But the overall accuracy of the

CNN-based method is more acceptable and accurate than the linear regression method. All these evaluation results demonstrate that deep learning methods can successfully reconstruct an acceptable accurate downscaling GRACE TWS data.

In the comparison study, VDSR shows the best performance. There are several possible reasons of this results. The main reason might be VDSR model was trained with more training samples than RCAN and has deeper architectures than SRCNN.

RCAN is a relatively state-of-the-art method in term of the data input process. All information required for resolution enhancements directly from the LR input without further interpolated to the size of HR target imagery. Meanwhile, RCAN used significantly few data to train the model. That could be another reason of the relatively poor performance.

In term of the computational efficiency and accuracy, all these three models have different performance. As shown in Table 1, VDSR takes the longest time (280 hours of 10,000 epochs) to train the model. Training SRCNN and RCAN took 28 hours and 106 hours, respectively. RCAN used about 24 times less data to train the model. Therefore, directly compare the time consuming of training each model is unfair. Given that, the number of trainable parameters was counted, which can reveal the complexity and efficiency of each model. As shown in Table 1, RCAN has the most trainable parameters, which means with the same train set training RCAN will cost much more time. According to the comparison of accuracy and efficiency of each model in Table 1, we can conclude that these three methods have their own advantages. The method should be selected according to the actual scenarios. For example, if the efficiency is the most important factor, SRCNN is the best choice. If the accuracy is the most important and large volume data is available for model training, VDSR is the best one. While, if only few data can be accessed for training and higher accuracy is required, RCAN or other state-of-the-art methods, such as SAN (Dai et al. 2019) and RFANet (Liu et al. 2020), are more suitable.

The uncertainties related to downscaling methods in this research are attributed to the following reasons. For the linear regression-based method, one linear relationship used for 121 (11*11) pixels may result in uncertainties because of the variation amongst 121 pixels. In addition to that, only 158 pairs of data were used to construct each regression equation, which also cannot precisely model the relationship between EALCO TWS and GRACE TWS. The performance of the linear regression-based method is also affected by the quantity and quality of samples for relationship establishment. For CNN-based methods, the adaption or domain transferring among EALCO TWS data (train data) and GRACE TWS data may introduce uncertainties into the downscaled results. But the uncertainties are expected to be decreased with more data. Therefore, for both methods, the higher qualified results are expected to generate with the increasing number of high-quality paired TWS data. Though the validation of TWS is restricted by the limited number of in-situ measurements, the downscaling methods in this study have been evaluated against the GRACE TWS products, indicating the robust of the adopted statistical method.

Conclusion

In this study, we developed a CNN-based framework to downscale the GRACE TWS data from 110 km resolution to 10 km resolution using simulations from the EALCO model. Compared to the traditional linear regression model, this framework performs better and improves spatial resolution with a factor of 11. Our study is the first to downscale national GRACE TWS using deep learning networks, which highlights the potential of the CNN-based super-resolution methods for predicting large-scale TWS and motivates further research to understand global water storage changes.

Our results demonstrated that, with limited training data, VDSR shows the high accuracy in GRACE TWS data downscaling. Apart from conventional methods, SRCNN is the most efficient method. There is no denying that the linear regression-based downscaling method is very competitive since it has no limitation on the downscaling ratio given qualified high-resolution data with acceptable quality. Moreover, acceptable results over Canada can be obtained using the linear regression-based method. The poor performance within the westernmost region of Canada and the Arctic Circle is also reasonable since these areas are undergone water loss due to melting glacier and permanent snow, which are not components of EALCO TWS (Wang and Li 2016). However, for the poor performance in the middle of Saskatchewan and low R^2 in the center of Canada, it is unexpected and unreasonable, which needs to be further analyzed. In addition, conspicuous Mach bands also show the insufficiency of the linear regression-based downscaling method in spatial downscaling based on accessible data. Also, the linear regression-based method was used based on several assumptions

mentioned in the former section. In contrast, the completely data-driven manner made CNN-based methods are better than linear regression in terms of flexibility and accuracy.

More auxiliary data with more detailed texture information, such as Digital Elevation Model (DEM) or precipitation data, could contribute both deep learning-based downscaling methods (Sun and Tang 2020; Vandal et al. 2017) and conventional statistic downscaling methods (Yin et al. 2018). With the aid of those data, deep learning-based spatial downscaling methods, especially the CNN-based methods, would perform better. Meanwhile, the accuracy evaluation could be done successfully (Sun and Tang 2020). Their optimal performance and capability in spatial downscaling applications could generate higher quality results without the limitation from downscaling ratio.

Acknowledgments

The authors would like to thank NASA GRACE for their publicly available data.

Funding

The work presented in this paper was supported by Natural Resources Canada [No. NRCan-5000050481]. The first author also acknowledges the China Scholarship Council for their support via a doctoral scholarship [No. 201906180088].

ORCID

Shusen Wang http://orcid.org/0000-0003-1860-899X
Jonathan Li http://orcid.org/0000-0001-7899-0049

References

Alexakis, D.D., and Tsanis, I.K. 2016. "Comparison of multiple linear regression and artificial neural network models for downscaling TRMM precipitation products using MODIS data." *Environmental Earth Sciences*, Vol. 75: pp. 1077.

Amthor, J.S., Chen, J.M., Clein, J., Frolking, S.E., Goulden, M.L., Grant, R.F., Kimball, J.S., et al. 2001. "Boreal forest CO_2 and water vapour exchanges predicted by nine ecosystem process models: Model results and relationships to measured fluxes." *Journal of Geophysical Research: Atmospheres*, Vol. 106: pp. 33623–33648.

Baño-Medina, J., Manzanas, R., and Gutiérrez, J.M. 2020. "Configuration and intercomparison of deep learning neural models for statistical downscaling." *Geoscientific Model Development Discussions*, Vol. 13(No. 4): pp. 2109–2124.

Chen, L., He, Q., Liu, K., Li, J., and Jing, C. 2019. "Downscaling of GRACE-derived groundwater storage based on the random forest model." *Remote Sensing*, Vol. 11(No. 24): pp. 2979.

Chen, N., Sui, L., Zhang, B., He, H., Junior, J.M., and Li, J. 2020. "Single satellite imagery super-resolution based on hybrid non-local similarity constrained convolution sparse coding." *IEEE Journal of Selected Topics in Appied Earth Observations and Remote Sensing*. Advance online publication. https://doi.org/10.1109/JSTARS.2020.3028774

Cooley, S., and Landerer, F. 2019. GRACE-FO Mission Documentation. PO.DAAC / JPL / NASA. [online] Physical Oceanography Distributed Active Archive Center (PO.DAAC). Accessed 17 July 2021, https://podaac.jpl.nasa.gov/gravity/gracefodocumentation

Coulibaly, P., Dibike, Y.B., and Anctil, F. 2005. "Downscaling precipitation and temperature with temporal neural networks." *Journal of Hydrometeorology*, Vol. 6(No. 4): pp. 483–496.

Dai, T., Cai, J., Zhang, Y., Xia, S. T., and Zhang, L. 2019. "Second-order attention network for single image super-resolution." Proceedings of the IEEE conference on computer vision and pattern recognition, pp. 11065–11074.

De Kauwe, M., Medlyn, B.E., Zaehle, S., Walker, A.P., Dietze, M.C., Wang, Y.-P., Luo, Y., et al. 2014. "Where does the carbon go? A model-data intercomparison of vegetation carbon allocation and turnover processes at two temperate forest free-air CO2 enrichment sites." *The New Phytologist*, Vol. 203(No. 3): pp. 883–899.

Dong, C., Loy, C.C., He, K., and Tang, X. 2016. "Image super-resolution using deep convolutional networks." *IEEE Transactions on Pattern Analysis and Machine Intelligence*, Vol. 38(No. 2): pp. 295–307.

Dong, C., Loy, C. C., and Tang, X. 2016. "Accelerating the super-resolution convolutional neural network." In *Proceedings of ECCV*, pp. 391–407. Cham: Springer.

Ducournau, A., and Fablet, R. 2016. "Deep learning for ocean remote sensing: an application of convolutional neural networks for super-resolution on satellite-derived SST data." 2016 9th IAPR Workshop on Pattern Recognition in Remote Sensing (PRRS), pp. 1–6. IEEE.

Eicker, A., Schumacher, M., Kusche, J., Döll, P., and Schmied, H.M. 2014. "Calibration/data assimilation approach for integrating GRACE data into the WaterGAP Global Hydrology Model (WGHM) using an ensemble Kalman filter: First results." *Surveys in Geophysics*, Vol. 35(No. 6): pp. 1285–1309.

Fok, H.S., and He, Q. 2018. "Water level reconstruction based on satellite gravimetry in the Yangtze River Basin." *ISPRS International Journal of Geo-Information*, Vol. 7(No. 7): pp. 286.

Frappart, F., Ramillien, G., and Ronchail, J. 2013. "Changes in terrestrial water storage versus rainfall and discharges in the Amazon basin." *International Journal of Climatology*, Vol. 33(No. 14): pp. 3029–3046.

Grant, R.F., Arain, A., Arora, V., Barr, A., Black, T.A., Chen, J., Wang, S., Yuan, F., and Zhang, Y. 2005. "Intercomparison of techniques to model high temperature effects on CO_2 and energy exchange in temperate and boreal coniferous forests." *Ecological Modelling*, Vol. 188(No. 2–4): pp. 217–252.

Grant, R.F., Barr, A.G., Black, T.A., Margolis, H.A., Dunn, A.L., Metsaranta, J., Wang, S., McCaughey, J.H., and Bourque, C.A. 2009. "Interannual variation in net

ecosystem productivity of Canadian forests as affected by regional weather patterns – a Fluxnet-Canada synthesis." *Agricultural and Forest Meteorology*, Vol. 149(No. 11): pp. 2022–2039.

Grant, R.F., Zhang, Y., Yuan, F., Wang, S., Hanson, P.J., Gaumont-Guay, D., Chen, J., et al. 2006. "Intercomparison of techniques to model water stress effects on CO_2 and energy exchange in temperate and boreal deciduous forests." *Ecological Modelling*, Vol. 196(No. 3–4): pp. 289–312.

Gustafsson, N., Janjić, T., Schraff, C., Leuenberger, D., Weissmann, M., Reich, H., Brousseau, P., et al. 2018. "Survey of data assimilation methods for convective-scale numerical weather prediction at operational centres." *Quarterly Journal of the Royal Meteorological Society*, Vol. 144(No. 713): pp. 1218–1256.

Hanson, P.J., Amthor, J.S., Wullschleger, S.D., Wilson, K.B., Grant, R.F., Hartley, A., Hui, D., et al. 2004. "Oak forest carbon and water simulations: model intercomparisons and evaluations against independent data." *Ecological Monographs.*, Vol. 74(No. 3): pp. 443–489.

He, K., Zhang, X., Ren, S., and Sun, J. 2016. "Deep residual learning for image recognition." Proceedings of the IEEE Conference on Computer Vision and Pattern Recognition, pp. 770–778. IEEE.

Jing, W., Yang, Y., Yue, X., and Zhao, X. 2016. "A comparison of different regression algorithms for downscaling monthly satellite-based precipitation over North China." *Remote Sensing*, Vol. 8(No. 10):pp. 835.

Keshk, H.M., Abdel-Aziem, M.M., Ali, A.S., and Assal, M.A. 2014, August. "Performance evaluation of quality measurement for super-resolution satellite images." Proceedings of 2014 Science Information Conferecnce, IEEE, Vol. 6(No. 2): pp. 364–371.

Kim, J., Lee, J. K., and Lee, K. M. 2016a. "Accurate image super-resolution using very deep convolutional networks." Proceedings of the IEEE Conference on Computer Vision and Pattern Recognition, pp. 1646–1654.

Kim, J., Lee, J. K., and Lee, K. M. 2016b. "Deeply-recursive convolutional network for image super-resolution." Proceedings of the IEEE Conference on Computer Vision and Pattern Recognition, pp. 1637–1645.

Kordpour, I., Farzaneh, S., and Shahhoseini, R. 2019. "Drought assessment of Iran using the MDI index." *The International Archives of the Photogrammetry, Remote Sensing and Spatial Information Sciences*, Vol. XLII-4/W18: pp. 659–663.

Lai, W.S., Huang, J.B., Ahuja, N., and Yang, M.H. 2017. "Deep Laplacian pyramid networks for fast and accurate super-resolution." Proceedings of the IEEE Conference on Computer Vision and Pattern Recognition, pp. 624–632.

Leblanc, M.J., Tregoning, P., Ramillien, G., Tweed, S.O., and Fakes, A. 2009. "Basin-scale, integrated observations of the early 21st century multiyear drought in southeast Australia." *Water Resources Research*, Vol. 45(No. 4): W04408.

Ledig, C., Theis, L., Huszár, F., Caballero, J., Cunningham, A., Acosta, A., Aitken, A., et al. 2017. "Photo-realistic single image super-resolution using a generative adversarial network." Proceedings of the IEEE Conference on Computer Vision and Pattern Recognition, pp. 4681–4690.

Lee, E., Županski, M., Županski, D., and Park, S.K. 2017. "Impact of the OMI aerosol optical depth on analysis increments through coupled meteorology–aerosol data assimilation for an Asian dust storm." *Remote Sensing of Environment.*, Vol. 193: pp. 38–53.

Lezzaik, K., and Milewski, A. 2018. "A quantitative assessment of groundwater resources in the Middle East and North Africa region." *Hydrogeology Journal*, Vol. 26(No. 1): pp. 251–266.

Li, J., Wang, S., and Zhou, F. 2016. "Time series analysis of long-term terrestrial water storage over Canada from GRACE satellites using principal component analysis." *Canadian Journal of Remote Sensing.*, Vol. 42(No. 3): pp. 161–170.

Lim, B., Son, S., Kim, H., Nah, S., and Mu Lee, K. 2017. "Enhanced deep residual networks for single image super-resolution." Proceedings of the IEEE Conference on Computer Vision and Pattern Recognition Workshops, pp. 136–144.

Liu, J., Zhang, W., Tang, Y., Tang, J., and Wu, G. 2020. "Residual feature aggregation network for image super-resolution." Proceedings of the IEEE/CVF Conference on Computer Vision and Pattern Recognition, pp. 2359–2368.

Long, D., Longuevergne, L., and Scanlon, B.R. 2014. "Uncertainty in evapotranspiration from land surface modeling, remote sensing, and GRACE satellites." *Water Resources Research*, Vol. 50(No. 2): pp. 1131–1151.

Long, D., Yang, Y., Wada, Y., Hong, Y., Liang, W., Chen, Y., Yong, B., Hou, A., Wei, J., and Chen, L. 2015. "Deriving scaling factors using a global hydrological model to restore GRACE total water stroage changes for China's Yangtze River Basin." *Remote Sensing of Environment.*, Vol. 168: pp. 177–193.

Ma, S., Wu, Q., Wang, J., and Zhang, S. 2017. "Temporal evolution of regional drought detected from GRACE TWSA and CCI SM in Yunnan Province." *Remote Sensing*, Vol. 9(No. 11): pp. 1124.

Macedo, H.E., Beighley, R.E., David, C.H., and Reager, J.T. 2019. "Using GRACE in a streamflow recession to determine drainable water storage in the Mississippi River basin." *Hydrology and Earth System Sciences*, Vol. 23(No. 8): pp. 3269–3277.

Mao, X. J., Shen, C., and Yang, Y. B. 2016. "Image restoration using convolutional auto-encoders with symmetric skip connections." Advances in Neural Information Processing Systems (NIPS), Vol. 29: pp. 2802–2810.

Medlyn, B.E., Zaehle, S., De Kauwe, M.G., Walker, A.P., Dietze, M.C., Hanson, P., Hickler, T., et al. 2015. "Using ecosystem experiments to improve vegetation models." *Nature Climate Change*, Vol. 5(No. 6): pp. 528–534.

Milewski, A.M., Thomas, M.B., Seyoum, W.M., and Rasmussen, T.C. 2019. "Spatial Downscaling of GRACE TWSA data to identify spatiotemporal groundwater level trends in the upper Floridan aquifer, Georgia, USA." *Remote Sensing*, Vol. 11: pp. 2756.

Miro, M.E., and Famiglietti, J.S. 2018. "Downscaling GRACE remote sensing datasets to high-resolution groundwater storage change maps of California's central valley." *Remote Sensing*, Vol. 10(No. 1): pp. 143.

Muskett, R.R., and Romanovsky, V.E. 2009. "Groundwater storage changes in arctic permafrost watersheds from GRACE and in situ measurements." *Environmental Research Letters*, Vol. 4(No. 4): pp. 045009.

Ning, S., Ishidaira, H., and Wang, J. 2014. "Statistical downscaling of GRACE-derived terrestrial water storage using satellite and GLDAS products." *Journal of Japan Society of Civil Engineers, Ser. B1)*, Vol. 70(No. 4): pp. 133–138.

Potter, C.S., Wang, S., Nikolov, N.T., McGuire, A.D., Liu, J., King, A.W., Kimball, J.S., et al. 2001. "Comparison of boreal ecosystem model sensitivity to variability in climate and forest site parameters." *Journal of Geophysical Research: Atmospheres*, Vol. 106: pp. 33671–33687.

Rahaman, M.M., Thakur, B., Kalra, A., Li, R., and Maheshwari, P. 2019. "Estimating high-resolution groundwater storage from GRACE: A random forest approach." *Environments*, Vol. 6(No. 6): pp. 63.

Reager, J.T., and Famiglietti, J.S. 2009. "Global terrestrial water storage capacity and flood potential using GRACE." *Geophysical Research Letters*, Vol. 36: pp. L23402.

Reager, J.T., Thomas, B.F., and Famiglietti, J.S. 2014. "River basin flood potential inferred using GRACE gravity observations at several months lead time." *Nature Geoscience*, Vol. 7(No. 8): pp. 588–592.

Riegger, J., and Tourian, M.J. 2014. "Characterization of runoff-storage relationships by satellite gravimetry and remote sensing." *Water Resources Research*, Vol. 50(No. 4): pp. 3444–3466.

Rocha Rodrigues, E., Oliveira, I., Cunha, R., and Netto, M. 2018. "DeepDownscale: A deep learning strategy for high-resolution weather forecast." 2018 IEEE 14th International Conference on e-Science (e-Science), pp. 415–422. IEEE. Available at: http://dx.doi.org/10.1109/escience.2018.00130.

Salimi, A.H., Masoompour Samakosh, J., Sharifi, E., Hassanvand, M.R., Noori, A., and von Rautenkranz, H. 2019. "Optimized artificial neural networks-based methods for statistical downscaling of gridded precipitation data." *Water*, Vol. 11(No. 8): pp. 1653.

Schmidhuber, J. 2015. "Deep learning in neural networks: An overview." *Neural Networks*, Vol. 61: pp. 85–117.

Schoof, J.T., and Pryor, S.C. 2001. "Downscaling temperature and precipitation: a comparison of regression-based methods and artificial neural networks." *International Journal of Climatology*, Vol. 21(No. 7): pp. 773–790.

Seyoum, W.M., and Milewski, A.M. 2016. "Monitoring and comparison of terrestrial water storage changes in the Northern High Plains using GRACE and *in-situ* based integrated hydrologic model estimates." *Advances in Water Resources*, Vol. 94: pp. 31–44.

Shamsudduha, M., Taylor, R.G., Jones, D., Longuevergne, L., Owor, M., and Tindimugaya, C. 2017. "Recent changes in terrestrial water storage in the Upper Nile Basin: an evaluation of commonly used gridded GRACE products." *Hydrology and Earth System Sciences*, Vol. 21(No. 9): pp. 4533–4549.

Shermeyer, J., and Van Etten, A. 2019. "The effects of super-resolution on object detection performance in satellite imagery." 2019 IEEE/CVF Conference on Computer Vision and Pattern Recognition Workshops (CVPRW), pp. 1432–1441. IEEE.

Shi, W., Caballero, J., Huszár, F., Totz, J., Aitken, A. P., Bishop, R., Rueckert, D., and Wang, Z. 2016. "Real-time single image and video super-resolution using an efficient sub-pixel convolutional neural network." Proceedings of the IEEE Conference on Computer Vision and Pattern Recognition, pp. 1874–1883.

Song, H.A., and Lee, S.-Y. 2013. "Hierarchical representation using NMF." International Conference on Neural Information Processing, pp. 466–473. Berlin, Heidelberg: Springer.

Sproles, E.A., Leibowitz, S.G., Reager, J.T., Wigington, P.J., Famiglietti, J.S., and Patil, S.D. 2015. "GRACE storage-runoff hysteresis reveal the dynamics of regional watersheds." *Hydrology and Earth System Sciences*, Vol. 19(No. 7): pp. 3253–3272.

Sun, A.Y. 2013. "Predicting groundwater level changes using GRACE data." *Water Resources Research*, Vol. 49(No. 9): pp. 5900–5912.

Sun, A.Y., and Tang, G. 2020. "Downscaling satellite and reanalysis precipitation products using attention-based deep convolutional neural nets." *Frontiers in Water*, Vol. 2: pp. 536743.

Tai, Y., Yang, J., and Liu, X. 2017. "Image super-resolution via deep recursive residual network." Proceedings of the IEEE Conference on Computer Vision and Pattern Recognition, pp. 3147–3155.

Thomas, A.C., Reager, J.T., Famiglietti, J.S., and Rodell, M. 2014. "A GRACE-based water storage deficit approach for hydrological drought characterization." *Geophysical Research Letters*, Vol. 41(No. 5): pp. 1537–1545.

Tomassetti, B., Verdecchia, M., and Giorgi, F. 2009. "NN5: A neural network based approach for the downscaling of precipitation fields – model description and preliminary results." *Journal of Hydrology*, Vol. 367(No. 1–2): pp. 14–26.

Tong, T., Li, G., Liu, X., and Gao, Q. 2017. "Image super-resolution using dense skip connections." Proceedings of the IEEE International Conference on Computer Vision, pp. 4799–4807.

Toth, C., and Jóźków, G. 2016. "Remote sensing platforms and sensors: A survey." *ISPRS Journal of Photogrammetry and Remote Sensing*, Vol. 115: pp. 22–36.

Vandal, T., Kodra, E., Ganguly, S., Michaelis, A., Nemani, R., and Ganguly, A. R. 2017. "DeepSD: Generating high resolution climate change projections through single image super-resolution." Proceedings of the 23rd ACM SIGKDD International Conference on Knowledge Discovery and Data Mining, pp. 1663–1672.

Voss, K.A., Famiglietti, J.S., Lo, M., Linage, C., de Rodell, M., and Swenson, S.C. 2013. "Groundwater depletion in the Middle East from GRACE with implications for transboundary water management in the Tigris-Euphrates-Western Iran region." *Water Resources Research*, Vol. 49(No. 2): pp. 904–914.

Walker, A.P., Hanson, P.J., De Kauwe, M.G., Medlyn, B.E., Zaehle, S., Asao, S., Dietze, M., et al. 2014. "Comprehensive ecosystem model-data synthesis using multiple data sets at two temperate forest free-air CO_2 enrichment experiments: Model performance at ambient CO_2 concentration." *Journal of Geophysical Research: Biogeosciences*, Vol. 119(No. 5): pp. 937–964.

Wang, S. 2008. "Simulation of evapotranspiration and its response to plant water and CO_2 transfer dynamics." *Journal of Hydrometeorology*, Vol. 9(No. 3): pp. 426–443.

Wang, S. 2019. "Freezing temperature controls baseflow recession rate for cold region watersheds." *Water Resources Research*, Vol. 55(No. 12): pp. 10479–10493.

Wang, S., Huang, J., Li, J., Rivera, A., McKenney, D.W., and Sheffield, J. 2014. "Assessment of water budget for sixteen large drainage basins in Canada." *Journal of Hydrology.*, Vol. 512: pp. 1–15.

Wang, S., Huang, J., Yang, D., Pavlic, G., and Li, J. 2015. "Long-term water budget imbalances and error sources for cold region drainage basins." *Hydrological Processes*, Vol. 29(No. 9): pp. 2125–2136.

Wang, S., and Li, J. 2016. "Terrestrial water storage climatology for Canada from GRACE satellite observations in 2002-2014." *Canadian Journal of Remote Sensing.*, Vol. 42(No. 3): pp. 190–202.

Wang, S., McKenney, D.W., Shang, J., and Li, J. 2014. "A national-scale assessment of long-term water budget closures for Canada's watersheds." *Journal of Geophysical Research: Atmospheres*, Vol. 119(No. 14): pp. 8712–8725.

Wang, S., Pan, M., Mu, Q., Shi, X., Mao, J., Brümmer, C., Jassal, R.S., Krishnan, P., Li, J., and Black, T.A. 2015. "Comparing evapotran." *Journal of Hydrometeorology*, Vol. 16(No. 4): pp. 1540–1560.

Wang, S., and Russell, H. 2016. "Forecasting snowmelt-induced flooding using GRACE satellite data: A case study for the Red River watershed." *Canadian Journal of Remote Sensing.*, Vol. 42(No. 3): pp. 203–213.

Wang, S., Trishchenko, A.P., and Sun, X. 2007. "Simulation of canopy radiation transfer and surface albedo in the EALCO model." *Climate Dynamics*, Vol. 29(No. 6): pp. 615–632.

Wang, S., Yang, Y., Luo, Y., and Rivera, A. 2013. "Spatial and seasonal variations in evapotranspiration over Canada's landmass." *Hydrology and Earth System Sciences*, Vol. 17(No. 9): pp. 3561–3575.

Wang, S., Zhou, F., and Russell, H.A.J. 2017. "Estimating snow mass and peak river flows for the Mackenzie River basin using GRACE satellite observations." *Remote Sensing*, Vol. 9(No. 3): pp. 256.

Yang, W., Zhang, X., Tian, Y., Wang, W., Xue, J.-H., and Liao, Q. 2019. "Deep learning for single image super-resolution: A brief review." *IEEE Transactions on Multimedia*, Vol. 21(No. 12): pp. 3106–3121.

Yin, W., Hu, L., Zhang, M., Wang, J., and Han, S.-C. 2018. "Statistical downscaling of GRACE-derived groundwater storage using ET data in the North China Plain." *Journal of Geophysical Research: Atmospheres*, Vol. 123(No. 11): pp. 5973–5987.

Zaehle, S., Medlyn, B.E., De Kauwe, M.G., Walker, A.P., Dietze, M.C., Hickler, T., Luo, Y., et al. 2014. "Evaluation of 11 terrestrial carbon-nitrogen cycle models against observations from two temperate Free-Air CO2 Enrichment studies." *The New Phytologist*, Vol. 202(No. 3): pp. 803–822.

Zhang, Y., Li, K., Li, K., Wang, L., Zhong, B., and Fu, Y. 2018. "Image super-resolution using very deep residual channel attention networks." Proceedings of the European Conference on Computer Vision (ECCV), pp. 286–301. Cham: Springer.

Zhang, Y., Wang, S., Barr, A.G., and Black, T.A. 2008. "Impact of snow cover on soil temperature and its simulation in the EALCO model." *Cold Regions Science and Technology.*, Vol. 52(No. 3): pp. 355–370.